ACS Photonics

Article

pubs.acs.org/journal/apchd5

Mode Control of Random Laser Action Assisted by Whispering-Gallery-Mode Resonance

Tong-Ming Weng,† Tzu-Han Chang,† Chih-Pin Lu, Meng-Lin Lu, Ju-Ying Chen, Shih-Hao Cheng, Chuan-Hsien Nieh, and Yang-Fang Chen*

Department of Physics, National Taiwan University, Taipei 106, Taiwan

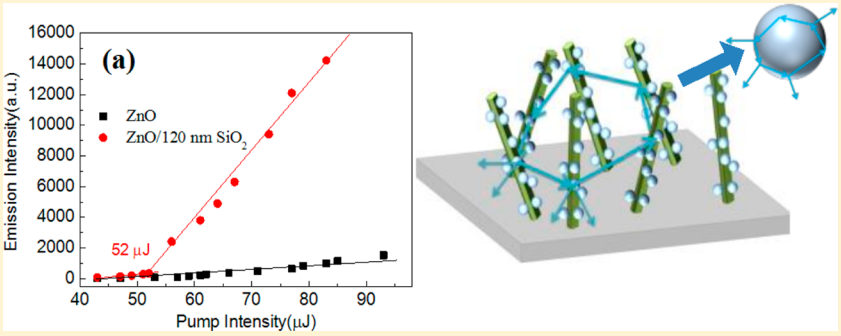

ABSTRACT: Whispering-gallery-mode (WGM) resonance manipulated random laser action has been proposed. To illustrate our working principle, lasing characteristics of ZnO nanorods decorated with SiO_2 nanospheres have been investigated. It is found that with the assistance of SiO_2 nanospheres the emission spectrum exhibits a very narrow background signal with a few sharp lasing peaks and a very small full width at half-maximum of less than 0.3 nm. The differential quantum efficiency (η_d) of random laser action can be greatly enhanced by up to 735%. More interestingly, the wavelength of laser action of ZnO nanorods can be controlled by the decoration of different-size nanospheres. The underlying origin is attributed to the fact that the decorated nanospheres not only enable the generation of WGM resonance and enhance the peak emission intensity but also can serve as scattering centers. Cathodoluminescence mapping images of nanorods decorated with nanospheres and theoretical calculation based on the spherical cavity were utilized to confirm our proposed mechanism. These intriguing features manifest the tunability of mode-controlled random laser action by WGM resonance of nanospheres. Our discovery shown here may open up a new approach for the creation of highly efficient optoelectronic devices.

KEYWORDS: *random laser, whispering-gallery-mode resonance, mode control*

In recent years, random lasing is a phenomenon that has been extensively investigated in some disordered media for its unique properties and potential applications,[1−5] since the original idea proposed by V. S. Letokhov.[1] Compared with conventional laser action due to Fabry−Perot resonance, random lasing necessitates no mirror cavities to achieve coherent feedback in the laser system in addition to its low-cost and simple process technology. Moreover, random lasing usually exhibits a very broad angular distribution, which is ideal for display applications. In random lasers, cavities are self-formed, and coherent and incoherent feedbacks can be provided by scattering events in the random medium.[1−7] As the close-loop is formed in the cavities and the gain exceeds the loss, random laser action can be achieved. A high gain medium and efficient light scattering centers are therefore required for the accomplishment of random lasing.

Recently many nanoscale optoelectronic devices have been extensively developed because of their low dimensionality and quantum confinement effect, such as transistors,[8,9] photodetectors,[10,11] and emitters.[12,13] Random lasing has also been widely studied in nanoscale materials such as nanorod arrays and nanocrystalline films.[14,15] ZnO, with a wide band gap of 3.37 eV, a high exciton binding energy of 60 meV, and many kinds of nanostructures, is very suitable for the fabrication of ultraviolet light-emitting diodes and laser devices with high efficiency.[16−18] In addition, due to a high refractive index in the ultraviolet region (∼2.5), the total internal reflection in ZnO structures can be easily achieved. On the basis of these favorable properties, conventional laser actions from ZnO nanostructures have been successfully demonstrated by Fabry−Perot cavities and different types of resonators.[19−21] However, according to previous studies,[22] the emission of ZnO nanorods (NRs) fabricated by a vapor−solid (VS) growth mechanism exhibits a very broad spectrum and the quantum efficiency of random laser action is rather poor.[5,15]

Here, we provide an alternative approach to overcome the above difficulty by the assistance of whispering-gallery-mode (WGM) resonance. To illustrate our working principle, the random lasing behavior arising from VS-ZnO NRs decorated by SiO_2 nanospheres has been investigated. WGM resonance has

Received: June 6, 2014
Published: November 17, 2014

been used to enhance the sensitivity of gas sensors, such as the detection of CO_2 and H_2O, and WGM lasing has also been demonstrated in several materials and circular structures.[23−26] In this study, it is found that after the nanosphere decoration the differential quantum efficiency can be greatly enhanced and the emission spectra show only very sharp peaks with a full width at half-maximum (fwhm) less than 0.3 nm and a very narrow background signal. Time-resolved photoluminescence (TRPL) experiments have also been performed to verify the induced laser action. Through varying SiO_2 nanosphere size, cathodoluminescence (CL) mapping, and theoretical calculation, we confirm that WGM is indeed the underlying mechanism responsible for the enhanced random laser action in SiO_2 nanospheres decorated VS-ZnO NRs. The unique feature of mode-controlled random laser action assisted by WGM resonance shown here should be very useful for the future development of highly efficient light-emitting devices.

RESULTS AND DISCUSSION

For the studied devices, a droplet of 2 μL of SiO_2 nanospheres (10 μM in ethanol) was deposited on VS-ZnO NRs. Three different sizes of SiO_2 nanospheres, with diameters of 120, 190, and 250 nm, were used. The morphology of the composite consisting of VS-ZnO NRs and SiO_2 nanospheres was characterized by scanning electron microscopy (SEM) (JSM 6500, JEOL). It is clearly seen in Figure 1 that VS-ZnO NRs have lengths of about 5−8 μm and diameters ranging between 100 and 500 nm. As shown in Figure 1a and b, the SiO_2 nanospheres with a diameter about 120 nm are deposited on VS-ZnO NRs as well as the substrate.

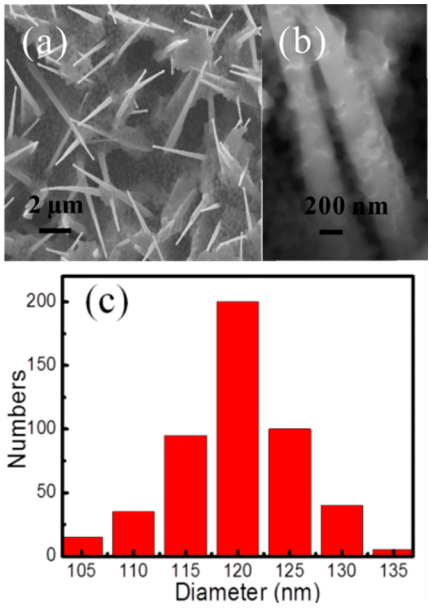

Figure 1. (a) Scanning electron microscope (SEM) image of ZnO nanorods decorated with SiO_2 nanospheres. (b) Enlarged SEM image of ZnO nanorods decorated with SiO_2 nanospheres. (c) Statistical bar chart of the size distribution of SiO_2 nanospheres.

The emission spectra of pristine VS-ZnO NRs under different pumping energy illuminated with a 266 nm pulsed laser are shown in Figure 2a. We observe only a very broad spontaneous emission spectrum at around 389 nm with a fwhm of about 12 nm, which is similar to a previous report.[15] As the pumping energy increases, the emission intensity increases gradually without any indication of laser action.

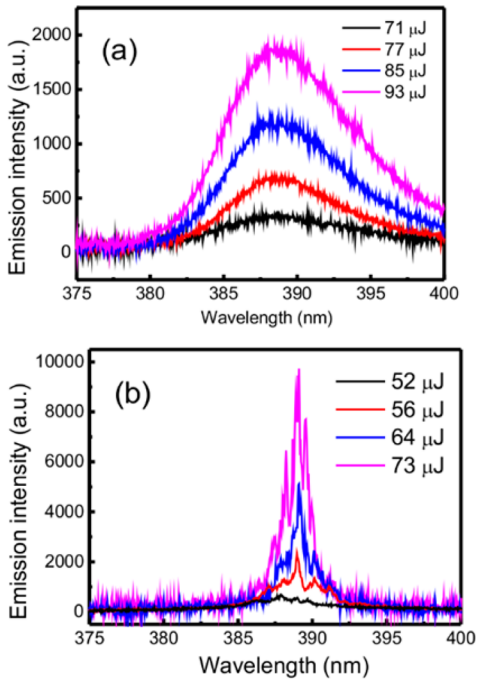

Figure 2. (a, b) Emission spectra of ZnO nanorods without and with the decoration of 120 nm SiO_2 nanospheres.

The emission spectrum of SiO_2 nanospheres decorated VS-ZnO NRs is shown in Figure 2b. Quite interestingly, after decorating with nanospheres, the fwhm of the whole emission spectrum is reduced to 1.9 nm. As the pumping energy increases, several sharp laser-like emission peaks superimposed on the broad spontaneous emission. We also found that the position and intensity of the sharp peaks randomly change at different moments, which is the inherent nature of random lasing behavior.[5,14] The emission characteristic of the randomly assembled VS-ZnO NRs as shown in Figure 2b can therefore be attributed to random laser action, which is achieved when specific frequencies of light are multiply amplified by stimulated emission in randomly closed loop paths.

To further examine the laser action, Figure 3a shows the analysis of the dependence of the emission intensity on pumping energy. Note that the emission intensity shown in Figure 3 represents the maximum peak value in the lasing

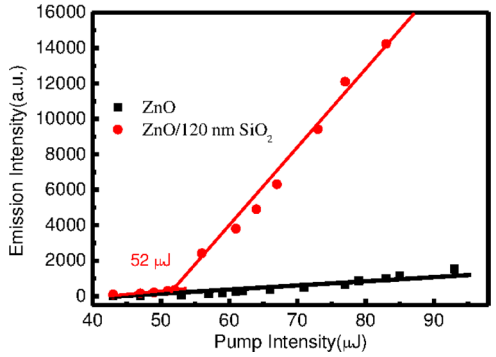

Figure 3. Plot of the emission intensity versus the pumping energy. Black boxes denote ZnO nanorods, and red circles denote pristine ZnO nanorods with the decoration of 120 nm SiO_2 nanospheres.

dx.doi.org/10.1021/ph500201b | ACS Photonics 2014, 1, 1258−1263

spectrum, and the angle between the collection of the laser emission and the pumping light beam is set at 30°. We can clearly see that there is an abrupt change of the slope, which provides a signature for the occurrence of stimulated emission. The value of the lasing threshold is approximately 52 μJ, implying that the laser action can be easily achieved compared with previous reports.[22] The differential quantum efficiency (η_d), defined as photons emitted per radiative electron−hole pair recombination above the threshold, can be determined by $\eta_d = P_O/P_I$,[27] where P_O and P_I are the output and input pumping power, respectively. It is found that the differential quantum efficiency (η_d) of ZnO NRs decorated with 120 nm SiO_2 nanospheres is about 7.3 times larger than the efficiency without 120 nm SiO_2 nanospheres, as shown in Figure 3.

Let us now try to understand the hidden mechanisms for the induced laser action and high differential quantum efficiency as observed above. There are two main possible mechanisms for the improved lasing characteristics arising from the decoration with SiO_2 nanospheres. First, there is a large contrast in refractive index between SiO_2 nanospheres and air, and the surface of ZnO NRs becomes rougher after the SiO_2 nanosphere deposition. The emitted light beam can thus be strongly scattered by SiO_2 nanospheres, which makes light travel more randomly. Therefore, random laser action is more easily achieved, and the threshold pumping energy is reduced. Second, due to the total internal reflections of light at the circular boundary, the spherical-shaped dielectric cavity could support WGM resonance. Once ZnO NRs are pumped by laser, the emissive light will prefer to be incident into the SiO_2 nanospheres than air because the refractive index of a SiO_2 nanosphere is closer to that of ZnO NRs. After the occurrence of resonance in the SiO_2 nanospheres, the ratio of the emission between the resonant and nonresonant frequencies will be greatly enhanced with a reduced line width. Therefore, stimulated emission can be much easier to achieve when the light with resonant frequency propagates with a closed-loop path among ZnO NRs. Figure 4 illustrates the underlying mechanisms responsible for the enhanced laser action assisted by the decoration of SiO_2 nanospheres.

To explore the possibility that WGM resonance is indeed responsible for the enhanced laser action, we first examine the Q factor, which is an important parameter to describe a laser cavity. From the experimental data, the Q factor is estimated to be 760 by the definition $Q = \lambda/\Delta\lambda$, where λ is the peak wavelength and $\Delta\lambda$ is the line width of the peak. Considering the WGM in a spherical cavity, the Q factor can be determined by the following equation:[28]

$$Q = \frac{\sqrt{3}\,\pi D m n R^{m/4}}{2\lambda(1 - R^{m/2})}\sin\left(\frac{2\pi}{m}\right) \quad (1)$$

where D is the diameter of the SiO_2 nanospheres, m is an integer, R is the reflectivity of the boundary, and n is the refractive index. If the experimentally obtained Q factor and m = 6 (for WGM) are inserted into the equation, the reflectivity is 99.6%. For a WGM cavity, it is in good agreement with the total internal reflection on the boundary of SiO_2 nanospheres. Interestingly, the integer m = 6 corresponds to the angle 60° required for the occurrence of the total internal reflection when a SiO_2 nanosphere is exposed to air. The corresponding angle of the incident light beam from the ZnO nanorod into a SiO_2 nanosphere is 44.7°.

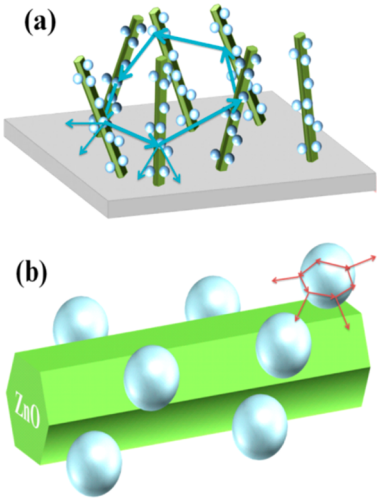

Figure 4. Schematic illustration of the mechanisms responsible for the enhanced laser action in SiO_2 nanospheres decorated ZnO nanorods. (a) SiO_2 nanospheres serve as scattering centers to assist light traveling in a randomly closed loop. (b) SiO_2 nanosphere serves as an excellent spherical cavity for the occurrence of whispering-gallery-mode resonance.

Second, we theoretically calculate the resonant WGMs arising from a nanoscale SiO_2 spherical cavity.[29] The main idea is that a light wave interferes with itself when having completed one full circulation within the resonator of SiO_2 nanospheres. In order to generate constructive interference, the total phase shift of the wave along its path has to be an integer multiple of 2π. Taking into account the polarization-dependent negative phase shift that occurs during the process of total internal reflection, we obtain the following equation by considering the condition of a spherical cavity:[25]

$$R_i = \frac{\lambda}{m_2\pi}\left[N + \frac{2}{\theta_i}\tan^{-1}\left(\beta\sqrt{m_2^2\tan^2\theta_i - m_1^2\csc^2\theta_i}\right)\right] \quad (2)$$

The factors m_1 and m_2 are the reflective indices of air and SiO_2 nanospheres, respectively. β depends on the polarization of the light wave; that is, for the TM polarization $\beta_{TM} = m_2^{-1}$ and for the TE polarization $\beta_{TE} = m_2$. R_i is the geometric parameter, which is the diameter of SiO_2 nanospheres. θ_i is the angle of incidence of the circulating light. According to the theoretical calculation, the WGM for the TE polarization does not exist, which is consistent with the previous investigation of laser action in a cylindrical cavity.[25] For 120 nm SiO_2 nanospheres, the TM-resonance peak position obtained by the theoretical calculation is approximately at 389 nm for N = 1. It is in good agreement with the emission peak of SiO_2 nanospheres decorated ZnO NRs as observed in Figure 2. Moreover, TRPL experiments of the spontaneous emission by pristine ZnO nanorods and SiO_2/ZnO composite monitored at 389 nm are shown in Figure 5. While the spontaneous emission exhibits a biexponential decay with time constants of 798 ps and 2.56 ns, the stimulated emission shows shorter decay times of 516 ps and 2.09 ns. This result provides an additional evidence to support that the emssion from SiO_2 nanospheres decorated ZnO NRs is indeed assisted by WGM resonance, because the modification of the local density of states of the electromagnetic field due to cavity modes can be used to enhance the spontaneous emission rate (the Purcell effect[30]).

dx.doi.org/10.1021/ph500201b | ACS Photonics 2014, 1, 1258−1263

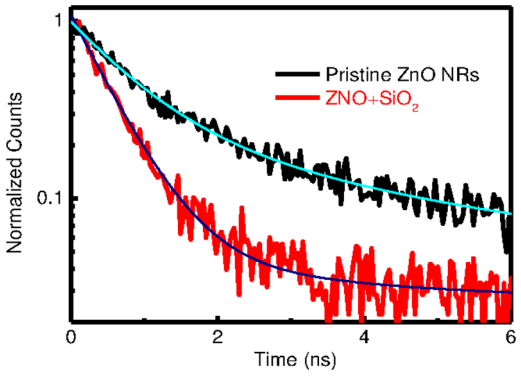

Figure 5. Time-resolved photoluminescence decay spectra with fitting curves for pristine ZnO nanorods and 120 nm SiO_2 nanospheres/ZnO nanorods monitored at the peak emission wavelength of 389 nm.

Note that in our experiment the excitation energy density to induce the laser action exceeds 10^7 W/cm^2, while for the TRPL measurements, the maximum excitation energy density used is 10^6 W/cm^2. Therefore, the experimental conditions of the TRPL for both decorated and undecorated ZnO nanorods are below the amplification threshold. The obtained lifetimes for the decorated and undecorated ZnO nanorods are of the same order of magnitude as reported previously.[31,32]

In order to further confirm the above proposed mechanisms for the observed laser action, different sizes of SiO_2 nanospheres decorated ZnO NRs have been investigated. Figure 6a and b show the emission spectra of the pristine ZnO NRs and ZnO NRs decorated by 190 and 250 nm SiO_2 nanospheres under the same pumping energy, respectively. Interestingly,

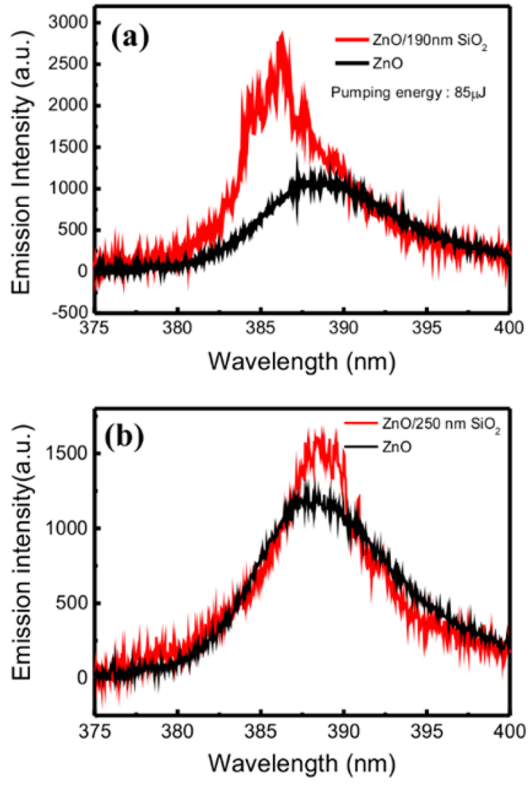

Figure 6. (a, b) Emission spectra of ZnO nanorods without and with decoration with 190 and 250 nm SiO_2 nanospheres under the same excitation power, respectively.

according to Figure 6a, we found that the amplified emission at particular wavelengths can still be observed with the position of sharp peaks centered approximately at 384 nm after the decoration with 190 nm SiO_2 nanospheres. The peak position is different from that of ZnO NRs decorated with 120 nm SiO_2 nanospheres. However, according to Figure 6b, after the decoration of 250 nm SiO_2 nanospheres, even though there exist several random lasing-like (amplified spontaneous emission) peaks compared to the pristine VS-ZnO NRs, they are not as pronounced as those of ZnO NRs decorated with 120 and 190 nm SiO_2 nanospheres. To investigate the effects of the size of decorated SiO_2 nanospheres on the amplified spontaneous emission of ZnO NRs, we have examined the resonant WGMs based on eq 2. As shown in Figure 7, it is

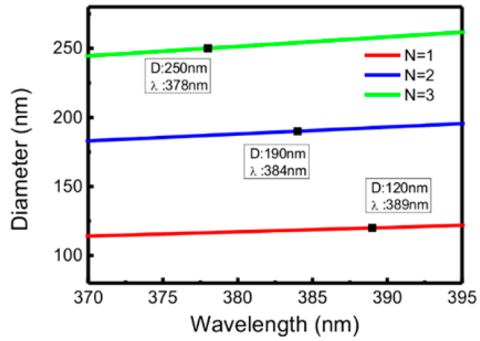

Figure 7. Plot of the diameter of spherical cavity versus TM-resonance peaks according to the therotical calculation given by eq 1. For 120 nm SiO_2 nanospheres, the TM-resonance peak position by the theoretical calculation is approximately at 389 nm for N = 1. For 190 nm SiO_2 nanospheres, the theoretical TM-resonance peak position is approximately at 384 nm for N = 2 (N = 1 is far above 600 nm). For 250 nm SiO_2 nanospheres, the theoretical TM-resonance peak position is at 378 nm for N = 3.

found that for the decoration of 190 nm SiO_2 nanospheres, the theoretical TM-resonance peak position for N = 1 is far away from our range of interest. But, for N = 2 the wavelength of WGM resonance is approximately at 384 nm, which is consistent with the position of the induced sharp peaks shown in Figure 6a. Because of a slight difference between the peak position of the WGM mode and ZnO emission spectrum, there is a less pronounced enhancement of the lasing action compared with that of the 120 nm SiO_2 nanospheres decorated ZnO NRs. For the decoration of 250 nm SiO_2 nanospheres, the nearest theoretical TM-resonance peak position to the ZnO emission spectrum is 378 nm with N = 3, which is too short compared with the wavelength of the main emission peak of ZnO NRs to have a significant influence. Besides, the order of the WGM mode is three, which is less effective in yielding laser action, too. Therefore, the blurred sharp peaks shown in Figure 6b can be attributed to the scattering effect induced by the decoration of nanospheres. Moreover, the normalized transmittance spectra have been performed for different-size SiO_2 nanospheres with the same density deposited on glass substrates, as shown in Figure 8. It is found that the transmittance has only a slight difference, implying the scattering effect is very similar. It supports the fact that WGM resonance plays a more important role than scattering effect in the induced stimulated emission due to the decoration of SiO_2 nanospheres.

dx.doi.org/10.1021/ph500201b | ACS Photonics 2014, 1, 1258−1263

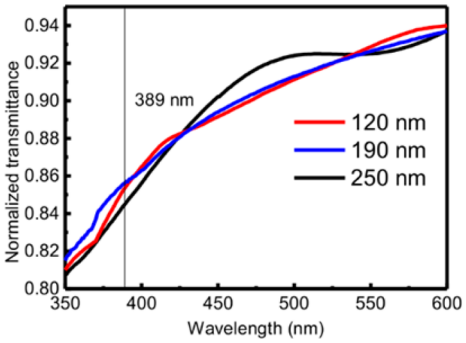

Figure 8. Transmittance spectra of SiO_2 nanospheres of three different sizes. It is clear that the transmittances for three different-size SiO_2 nanospheres around 389 nm exhibit only a slight difference.

Finally, Figure 9 shows the corresponding CL mapping image for ZnO NRs decorated with 120 and 190 nm SiO_2

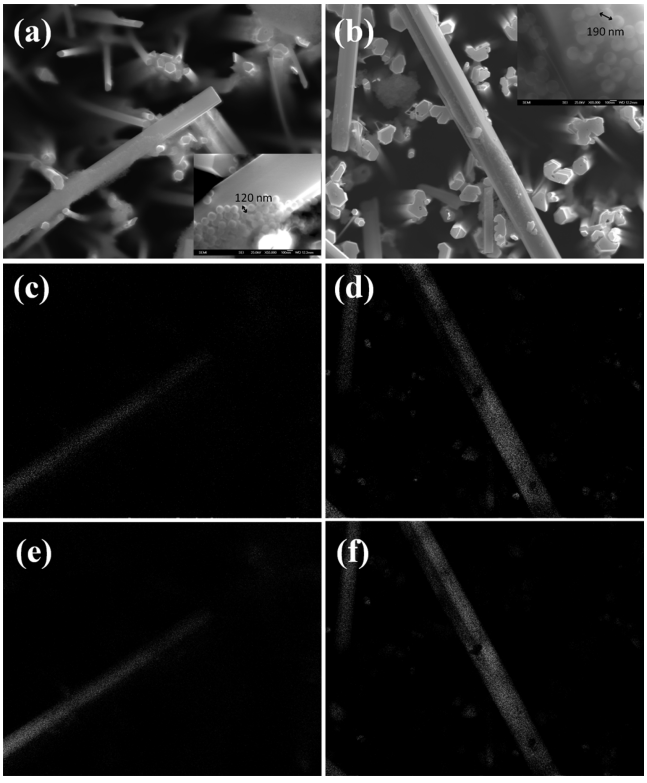

Figure 9. Scanning electron microscope image of ZnO nanorods decorated with (a) 120 nm and (b) 190 nm SiO_2 nanospheres. The embedded image shows the size of SiO_2 nanospheres. (c, d) Corresponding cathodoluminescence mapping images monitored at 384 nm for the sample decorated with 120 and 190 nm SiO_2 nanoparticles, respectively. (e, f) Corresponding cathodoluminescence mapping images monitored at 389 nm for the sample decorated with 120 and 190 nm SiO_2 nanoparticles, respectively.

nanospheres, in which the emissions at 384 and 389 nm are selected as the mapping wavelength. Comparing the SEM image shown in Figure 9a and b with the CL mapping image shown in Figure 9c, d, e, and f, it is clear that the bright emission comes from the location where the SiO_2 nanospheres were decorated on ZnO NRs for 120 nm SiO_2 nanospheres in Figure 9e and for 190 nm SiO_2 nanospheres in Figure 9d. As we can see for the sample decorated with 120 nm SiO_2 nanoparticles monitored at 384 nm, the CL image in Figure 9c exhibits the same brightness for the ZnO nanorods with and without SiO_2 nanoparticles. However, when the CL image is monitored at 389 nm (Figure 9e), the portion with SiO_2 nanoparticles is brighter than that without SiO_2 nanoparticles. In contrast, for the sample decorated with 190 nm SiO_2 nanoparticles monitored at 384 nm, the CL image in Figure 9d shows that the portion with SiO_2 nanoparticles is brighter than that without SiO_2 nanoparticles. However, when the CL image is monitored at 389 nm (Figure 9f), the emission of ZnO nanorods shows the same brightness for the portion with and without SiO_2 nanoparticles. The above result clearly supports the fact that WGM resonance is the underlying mechanism responsible for our observations.

CONCLUSION

In conclusion, a novel approach to manipulate random laser action based on WGM resonance has been demonstrated. It is found that the lasing characteristics can be improved significantly, including narrower emission spectra, sharper lasing peaks, smaller lasing threshold, and higher differential quantum efficiency. Moreover, we found that the lasing wavelength is tunable by the decoration of nanospheres with different sizes. Through CL mapping images and the theoretical calculation, we have firmly confirmed that the observed laser action in nanosphere-decorated ZnO NRs arises from the assistance of WGM resonance. These unique features manifest an enhanced random laser action with mode-controlled behavior. In general, our approach could be extended to many other composites consisting of nanoparticles and light-emitting materials. It therefore can open up a new route for the creation of highly efficient optoelectronic devices.

METHOD

The studied ZnO NRs in this work were fabricated by the VS growth mechanism.[33] A sapphire substrate was placed on the top of an alumina boat loaded with high-purity Zn powder (99.99%), and the whole alumina boat was located at the center of a tube furnace. Subsequently, the reaction chamber was evacuated and kept at a pressure of 10 Torr when argon and oxygen with a high purity of 99.9% were introduced into the reaction chamber at a flow rate of 200 and 5 sccm, respectively. In addition, the growth temperature was maintained at 620 °C, and the dwell time was 1 h. After the fabrication, VS-ZnO NRs were formed uniformly over the entire substrate.

To prepare the SiO_2 nanospheres, sodium silicate was mixed with sodium aluminate. After that, a 1.2 M H_2SO_4 solution was added drop-by-drop to neutralize that mixture to pH ~9. Then, the alumina silicate was mixed with C_{16}TMAB (cetyltrimethlammonium bromide 99% Merck) surfactant solution. The molar ratio of the gel is 1.0 SiO_2:0.028 $NaAlO_2$:0.71 C_{16}TMAB:0.6 NaOH:0.24 H_2SO_4:300 H_2O. The gel mixture was heated statically at 100 °C for 6 h in an autoclave. The as-synthesized product was filtrated and washed with deionized water, then calcined at 560 °C in air for 6 h to remove the organic templates, and the nanosized SiO_2 nanospheres were obtained. The diameter of the SiO_2 nanoparticles ranged from 105 to 135 nm.

To investigate random laser action, the samples were optically excited by a Q-switched Nd:yttrium aluminum garnet laser (266 nm, 3−5 ns pulse, 10 Hz) focused to a beam size about 200 μm in diameter. For the time-resolved photo-

dx.doi.org/10.1021/ph500201b | ACS Photonics 2014, 1, 1258−1263

luminescence, the excitation scource is a Ti-sapphire mode-locked laser (Coherent, Mira 900) with a repetition rate of 76 MHz and pulsewidth of 120 fs. The wavelength is tripled to 266 nm with an average power of 1 mW to pump the sample at room temperature. The TRPL signals were detected by a time-corrected single photon counting (Pico Harp 300) system with a time resolution of about 10 ps. The CL mapping images were carried out on the same SEM instrument equipped with Gatan-Mono-CL3 operating at 10 kV. All measurements were performed at room temperature.

AUTHOR INFORMATION

Corresponding Author

*E-mail: yfchen@phys.ntu.edu.tw.

Author Contributions

†T.-M. Weng and T.-H. Chang contributed equally to this work.

Notes

The authors declare no competing financial interest.

ACKNOWLEDGMENTS

This work was supported by the National Science Council and Ministry of Education of the Republic of China.

REFERENCES

(1) Letokhov, V. S. Generation of Light by a Scattering Medium with Negative Resonance Absorption. *Sov. Phys. JETP* **1968**, *26*, 1442−1452.

(2) Sun, B. Q.; Gal, M.; Gao, Q.; Tan, H. H.; Jagadish, C.; Puzzer, T.; Ouyang, L.; Zou, J. Epitaxially Grown GaAsN Random Laser. *J. Appl. Phys.* **2003**, *93*, 5855.

(3) Quochi, F. Random Lasers Based on Organic Epitaxial Nanofibers. *J. Opt.* **2010**, *12*, 024003.

(4) Guerin, W.; Mercadier, N.; Michaud, F.; Brivio, D.; Froufe-Perez, L. S.; Carminati, R.; Eremeev, V.; Goetschy, A.; Skipetrov, S. E.; Kaiser, R. Towards a Random Laser with Cold Atoms. *J. Opt.* **2010**, *12*, 024002.

(5) Cao, H.; Zhao, Y. G.; Ho, S. T.; Seelig, E. W.; Wang, Q. H.; Chang, R. P. H. Random Laser Action in Semiconductor Powder. *Phys. Rev. Lett.* **1999**, *82*, 2278−2281.

(6) Sznitko, L.; Cyprych, K.; Szukalski, A.; Miniewicz, A.; Mysliwiec, J. Coherent−Incoherent Random Lasing Based on Nano-rubbing Induced Cavities. *Laser Phys. Lett.* **2014**, *11*, 045801.

(7) Cao, H. Lasing in Random Media. *Waves Random Media* **2003**, *13*, R1−R39.

(8) Shaw, J. E.; Stavrinou, P. N.; Anthopoulos, T. D. On-Demand Patterning of Nanostructured Pentacene Transistors by Scanning Thermal Lithography. *Adv. Mater.* **2013**, *25*, 552−558.

(9) Kulmala, T. S.; Colli, A.; Fasoli, A.; Lombardo, A.; Haque, S.; Ferrari, A. C. Self-Aligned Coupled Nanowire Transistor. *ACS Nano* **2011**, *5*, 6910−6915.

(10) Lu, M. L.; Weng, T. M.; Chen, J. Y.; Chen, Y. F. Ultrahigh-Gain Single SnO_2 Nanowire Photodetectors Made with Ferromagnetic Nickel Electrodes. *NPG Asia Mater.* **2012**, *4*, e26.

(11) Lu, M. L.; Lai, C. W.; Pan, H. J.; Chen, C. T.; Chou, P. T.; Chen, Y. F. A Facile Integration of Zero-(I−III−VI Quantum Dots) and One-(Single SnO_2 Nanowire) Dimensional Nanomaterials: Fabrication of a Nanocomposite Photodetector with Ultrahigh Gain and Wide Spectral Response. *Nano Lett.* **2013**, *13*, 1920−1927.

(12) Fang, X.; Yan, J.; Hu, L.; Liu, H.; Lee, P. S. Thin SnO_2 Nanowires with Uniform Diameter as Excellent Field Emitters: A Stability of More than 2400 Minutes. *Adv. Funct. Mater.* **2012**, *22*, 1613−1622.

(13) Zhai, T.; Ye, M.; Li, L.; Fang, X.; Liao, M.; Li, Y.; Koide, Y.; Bando, Y.; Golberg, D. Single-Crystalline Sb_2Se_3 Nanowires for High-Performance Field Emitters and Photodetectors. *Adv. Mater.* **2010**, *22*, 4530−4533.

(14) Yu, S. F.; Yuen, C.; Lau, S. P.; Park, W. I.; Yi, G. C. Random Laser Action in ZnO Nanorod Arrays Embedded in ZnO Epilayers. *Appl. Phys. Lett.* **2004**, *84*, 3241−3243.

(15) Zhu, H.; Shan, C. X.; Zhang, J. Y.; Zhang, Z. Z.; Zhao, D. X.; Li, B. H.; Yao, B.; Shen, D. Z.; Fan, X. W.; Tang, Z. K.; Huo, X. H.; Choy, K. L. Low-Threshold Electrically Pumped Random Lasers. *Adv. Mater.* **2010**, *22*, 1877−1881.

(16) Tsukazaki, A.; Kubota, M.; Ohtomo, A.; Onuma, T.; Ohtani, K.; Ohno, H.; Chichibu, S. F.; Kawasaki, M. Blue Light-Emitting Diode Based on ZnO. *Jpn. J. Appl. Phys.* **2005**, *44*, L643−L645.

(17) Chu, S.; Olmedo, M.; Yang, Z.; Kong, J.; Liu, J. Electrically Pumped Ultraviolet ZnO Diode Lasers on Si. *Appl. Phys. Lett.* **2008**, *93*, 181106.

(18) Zhang, C.; Zhang, F.; Xia, T.; Kumar, N.; Hahm, J. I.; Liu, J.; Wang, Z. L.; Xu, J. Low-Threshold Two-Photon Pumped ZnO Nanowire Lasers. *Opt. Express* **2009**, *17*, 7893−7900.

(19) Huang, M. H.; Mao, S.; Feick, H.; Yan, H.; Wu, Y.; Kind, H.; Weber, E.; Russo, R.; Yang, P. Room-Temperature Ultraviolet Nanowire Nanolasers. *Science* **2001**, *292*, 1897−1899.

(20) Gargas, D. J.; Moore, M. C.; Ni, A.; Chang, S. W.; Zhang, Z.; Chuang, S. L.; Yang, P. Whispering Gallery Mode Lasing from Zinc Oxide Hexagonal Nanodisks. *ACS Nano* **2010**, *4*, 3270−3276.

(21) Chen, R.; Ling, B.; Sun, X. W.; Sun, H. D. Room Temperature Excitonic Whispering Gallery Mode Lasing from High-Quality Hexagonal ZnO Microdisks. *Adv. Mater.* **2011**, *23*, 2199−2204.

(22) Chen, Y. T.; Chen, Y. F. Enhanced Random Lasing in ZnO Nanocombs Assisted by Fabry−Perot Resonance. *Opt. Express* **2011**, *19*, 8728−8734.

(23) Chen, C. W.; Chen, Y. F. Whispering Gallery Modes in Highly Hexagonal Symmetric Structures of SBA-1 Mesoporous Silica. *Appl. Phys. Lett.* **2007**, *90*, 071104.

(24) Wu, Y.; Leung, P. T. Lasing Threshold for Whispering-Gallery-Mode Microsphere Lasers. *Phys. Rev. A* **1999**, *60*, 630−633.

(25) Lin, T. J.; Chen, H. L.; Chen, Y. F.; Cheng, S. Room-Temperature Nanolaser from CdSe Nanotubes Embedded in Anodic Aluminum Oxide Nanocavity Arrays. *Appl. Phys. Lett.* **2008**, *93*, 223903.

(26) Grudinin, I. S.; Matsko, A. B.; Maleki, L. Brillouin Lasing with a CaF_2 Whispering Gallery Mode Resonator. *Phys. Rev. Lett.* **2009**, *102*, 043902.

(27) Lu, M. L.; Lin, H. Y.; Chen, T. T.; Chen, Y. F. Random Lasing in the Composites Consisting of Photonic Crystals and Semiconductor Nanowires. *Appl. Phys. Lett.* **2011**, *99*, 091106.

(28) Bhowmik, A. K. Polygonal Optical Cavities. *Appl. Opt.* **2000**, *39*, 3071.

(29) Nobis, T.; Kaidashev, E.; Rahm, A.; Lorenz, M.; Grundmann, M. Whispering Gallery Modes in Nanosized Dielectric Resonators with Hexagonal Cross Section. *Phys. Rev. Lett.* **2004**, *93*, 103903.

(30) Purcell, E. M. Spontaneous Emission Probabilities at Radio Frequencies. *Phys. Rev.* **1946**, *69*, 681.

(31) Huang, M. H.; Mao, S.; Feick, H. Q.; Wu, Y. Y.; Kind, H.; Weber, E.; Russo, R.; Yang, P. D. Room-Temperature Ultraviolet Nanowire Nanolaser. *Science* **2001**, *292*, 1897−1899.

(32) Han, X. H.; Wang, G. Z.; Wang, Q. T.; Cao, L.; Liu, R. B.; Zou, B. S.; Hou, J. G. Ultraviolet Lasing and Time-Resolved Photoluminescence of Well-Aligned ZnO Nanorod Arrays. *Appl. Phys. Lett.* **2005**, *86*, 233106.

(33) Umar, A.; Kim, S. H.; Lee, Y. S.; Nahm, K. S.; Hahn, Y. B. Catalyst-Free Large-Quantity Synthesis of ZnO Nanorods by a Vapor−Solid Growth Mechanism: Structural and Optical Properties. *J. Cryst. Growth* **2005**, *282*, 131−136.